The General Circulation in a Dissipative Ocean Basin with Longshore Wind Stresses

JOHN A. T. BYE

The Flinders Institute for Atmospheric and Marine Sciences, The Flinders University of South Australia, Bedford Park, South Australia 5042

(Manuscript received 1 December 1982, in final form 27 May 1983)

ABSTRACT

Solutions of the Stommel equation are presented which take the form of free waves in the interior of the ocean basin, driven by convergences and divergences in coastal transports brought about by the variation of the longshore wind stress around the coast. These waves have been termed "coastal waves" and result from the beta-effect in the presence of a uniform frictional process, such as the loss of momentum by the ocean to the atmosphere. The coastal waves which typically transport 5 Sv extend significantly into the interior of the ocean from all boundaries except the western boundary, and also drive a westward nonlinear current, appear to be an important feature in the general circulation. A good example of a quasi-steady wavefield induced by intermediate-scale coastline geography occurs in the Flinders Current off the south coast of Australia.

The western boundary current, of course, compensates for imbalances in interior transport. Its structure results from forcing, both by this transport and the longshore wind stress on the western coast itself, which produces no net transport outside of the boundary layer.

1. Introduction

The general circulation of the oceans has been discussed extensively in the literature. In this paper, we examine the structure of the circulation in the interior of an ocean basin in which a uniform frictional process is assumed to operate; we also include forcing due to coastal currents driven by longshore wind stresses. It is shown that onshore and offshore transports are required to maintain the coastal currents force circulations, which are a response to the internal frictional process and the beta effect. These waves, called coastal waves, offer a natural description of the intermediate-scale structure of the general circulation in the interior of ocean basins. A good example of a quasi-steady wavefield forced by the longshore wind occurs in the Flinders Current off the south coast of Australia (Bye, 1971).

In addition, we examine the structure of the western boundary current, a consequence of forcing by 1) the wind stress curl and the longshore wind structure on the other boundaries of the ocean basin; and 2) the longshore wind structure on the western boundary itself.

2. The steady-state equations

The linearized steady-state transport equations are

$$-\rho_0 f\bar{v}h = \tau_{sx} - \tau_{Bx} + \frac{\partial}{\partial x}\bar{\tau}_{xx}h + \frac{\partial}{\partial y}\bar{\tau}_{xy}h - \frac{\partial \bar{p}h}{\partial x} + p_B\frac{\partial h_0}{\partial x} + p_0\frac{\partial \eta}{\partial x}, \quad (1)$$

$$\rho_0 f\bar{u}h = \tau_{sy} - \tau_{By} + \frac{\partial}{\partial x}\bar{\tau}_{yx}h + \frac{\partial}{\partial y}\bar{\tau}_{yy}h - \frac{\partial \bar{p}h}{\partial y} + p_B\frac{\partial h_0}{\partial y} + p_0\frac{\partial \eta}{\partial y}, \quad (2)$$

in which $0x$ is toward the east, $0y$ toward the north; the overbar denotes a depth average such that $\bar{\phi} = h^{-1}\int_{-h_0}^{\eta}\phi dz$, where $h = h_0 + \eta$ is the total depth, z vertically upward, η the surface elevation, and h_0 the undisturbed depth; $(\bar{u}, \bar{v})$ are velocity components, (τ_{sx}, τ_{sy}) is the surface shearing stress, (τ_{Bx}, τ_{By}) the bottom shearing stress, and (τ_{xx}, τ_{xy}) and (τ_{yx}, τ_{yy}) the components of lateral stress along $0x$ and $0y$, respectively; ρ_0 is a constant reference density for seawater; $f = 2\Omega\sin\phi$ is the Coriolis parameter, in which Ω is the angular speed of rotation of the Earth and ϕ latitude; p is pressure, p_B the bottom pressure, and p_0 the surface pressure.

The transport continuity equation is

$$\frac{\partial \bar{u}h}{\partial x} + \frac{\partial \bar{v}h}{\partial y} = 0. \quad (3)$$

In Eqs. (1) and (2) the shearing stresses will be assumed to have the form

$$(\tau_{sx}, \tau_{sy}) = (\tau_{wx}, \tau_{wy}) - \rho_0 C_0(u_0, v_0), \quad (4)$$

in which (τ_{wx}, τ_{wy}) is the wind stress, and the second term the understress (Bye, 1980); (u_0, v_0) is the surface current, and C_0 the understress coefficient. The understress is due to the dissipation of energy by the surface current in the air-sea boundary layer. The coefficient (C_0) has the form (Bye, 1980)

$$C_0 = \frac{\rho_a}{\rho_0} K|\underline{u}_a|(1 + \xi^2),$$

where ρ_a is the density of air, $\underline{u}_a$ the mean wind velocity with the associated drag coefficient K, and $\xi = (\overline{\underline{u}_0'^2})^{1/2}/|\underline{u}_0|$ the intensity of the oceanic surface two-dimensional turbulence, in which $\underline{u}_0'$ denotes a current fluctuation; C_0 is proportional to the wind speed, and significantly enhanced by the high turbulent intensity of the trajectories of the water particles which constitute the mean current. A typical magnitude for C_0 is 10^{-4} m s^{-1}.

The bottom stress is assumed to have the form

$$(\tau_{Bx}, \tau_{By}) = \rho_0 C_1(u_1, v_1), \tag{5}$$

where (u_1, v_1) is the bottom current, and C_1 the coefficient of bottom friction; the divergence of the lateral stress is assumed to have the usual forms;

$$\left.\begin{aligned} \frac{\partial}{\partial x}\bar{\tau}_{xx}h + \frac{\partial}{\partial y}\bar{\tau}_{xy}h &= \rho_0 K\nabla^2\bar{u}h \\ \frac{\partial}{\partial x}\bar{\tau}_{yx}h + \frac{\partial}{\partial y}\bar{\tau}_{yy}h &= \rho_0 K\nabla^2\bar{v}h \end{aligned}\right\}, \tag{6}$$

in which K is a constant coefficient of lateral diffusion. We also assume throughout that the surface pressure (p_0) is a constant and that $|\eta| \ll h_0$.

3. The ocean model

The ocean basin will be assumed to consist of two regions (Fig. 1): 1) the coastal zone which consists of the inner (continental) shelf ($h < h_T$) and the outer shelf ($h \geq h_T$); and 2) the ocean interior in which $h \geq h_T$ throughout, where h_T is the scale depth for the thermohaline circulation. For $h < h_T$ the flow is assumed to be barotropic such that $\underline{u}_0 = \bar{\underline{u}}$, and for $h \geq h_T$ the flow is assumed to be baroclinic with a zero horizontal pressure gradient at the bottom, such that $\underline{u}_0 = (h/h_T)\bar{\underline{u}}$ and $\underline{u}_1 = 0$. In reality, there would be a smooth variation between the flow regimes on the inner and the outer shelf and h_T would mark approximately the center of the transition zone.

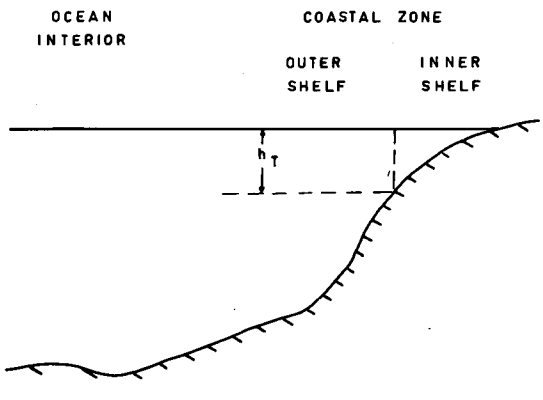

FIG. 1. The ocean model.

The vorticity equation for $h \geq h_T$, formed in a standard manner from (1) and (2), using (3)–(6), is

$$\beta\frac{\partial\psi}{\partial x} = \frac{1}{\rho_0}\left(\frac{\partial\tau_{wy}}{\partial x} - \frac{\partial\tau_{wx}}{\partial y}\right) - R\nabla^2\psi + K\nabla^4\psi, \tag{7}$$

where

$$\bar{v}h = \frac{\partial\psi}{\partial x}, \quad \bar{u}h = -\frac{\partial\psi}{\partial y}, \quad \beta = \frac{df}{dy},$$

and $R = C_0/h_T$. Note that since the understress acts on the surface current, the friction coefficient (R) involves the scale depth h_T. Limiting forms of (7) apply in each region of the ocean basin. We consider first the outer shelf of the coastal zone.

a. The coastal zone

We assume a meridional coast along which the y-derivatives may be neglected in comparison with the x-derivatives in the usual manner, and the wind stress is independent of the cross-shelf coordinate. Then on the outer shelf, the vorticity equation reduces to the boundary layer approximation to (7), namely,

$$\beta v_0 = -R\frac{\partial v_0}{\partial x} + K\frac{\partial^3 v_0}{\partial x^3}, \quad h \geq h_T. \tag{8}$$

On the inner shelf, from (1) and (2) and using (3)–(6), and again making the boundary layer approximation, we obtain

$$\beta v_0 = \frac{1}{\rho_0}\frac{\partial}{\partial x}\frac{\tau_{wy}}{h} - (C_0 + C_1)\frac{\partial}{\partial x}\left(\frac{v_0}{h}\right) + K\frac{\partial}{\partial x}\left(\frac{1}{h}\frac{\partial^2}{\partial x^2}v_0 h\right), \quad h < h_T. \tag{9}$$

Eqs. (8) and (9) may be combined to yield the single coastal zone equation

$$\beta v_0 = \frac{1}{\rho_0}\frac{\partial}{\partial x}\frac{\tau_{wy}}{h'} - Rh_T\frac{\partial}{\partial x}\left(\frac{v_0}{h'}\right) + K\frac{\partial}{\partial x}\left(\frac{1}{h'}\frac{\partial^2}{\partial x^2}v_0 h'\right), \tag{10}$$

where

$$\left.\begin{aligned} h' &= h, \quad h < h_T \\ h' &= h_T, \quad h \geq h_T \end{aligned}\right\},$$

and for simplicity $C_0 + C_1$ in (9) has been replaced by C_0, so that a uniform friction coefficient is assumed to apply throughout the coastal zone.

The frictional processes in (10) are represented by the dissipation time constant (R^{-1}), and the coefficient of lateral diffusion (K). We assume that they jointly give rise to a boundary layer width,

$$W \sim \frac{R}{\beta} \sim \left(\frac{K}{\beta}\right)^{1/3},$$

in which from dimensional reasoning,

$$K \sim RW^2. \tag{11}$$

Thus typically for $R = 10^{-6}$ s^{-1} and $W = 50$ km, we have $K = 3 \times 10^3$ m^2 s^{-1}. On nondimensionalizing (10) we obtain

$$V = \frac{\partial}{\partial X} F_y/H - \epsilon \frac{\partial}{\partial X} V/H + \epsilon^3 \frac{\partial}{\partial X} \frac{1}{H} \frac{\partial^2}{\partial X^2} VH, \tag{12}$$

in which

$$X = xL^{-1}, \quad Y = yL^{-1},$$

$$(F_x, F_y) = \left(\frac{\tau_{wx}}{\tau_0}, \frac{\tau_{wy}}{\tau_0}\right), \quad H = h'/h_T,$$

$V = v_0\rho_0\beta L h_T \tau_0^{-1}$ is the nondimensional meridional current, and $\epsilon = R/\beta L$. Eq. (12) which depends on only one small parameter (ϵ) is the model equation for the coastal zone.

b. *The ocean interior*

First, on assuming a scale (S) for the horizontal motion, and using (11), we have

$$\frac{K\nabla^4\psi}{R\nabla^2\psi} \approx \left(\frac{W}{S}\right)^2.$$

Hence in the ocean interior where $(W/S)^2 \ll 1$, the effect of lateral friction is small in comparison with that of understress, and (7) reduces to the Stommel equation. On nondimensionalizing, in a manner similar to (10), we obtain the model equation for the ocean interior,

$$\frac{\partial \phi}{\partial X} = \frac{\partial F_y}{\partial X} - \frac{\partial F_x}{\partial Y} - \epsilon\nabla^2\phi, \tag{13}$$

where

$$\phi = \rho_0\beta\psi/\tau_0.$$

Solutions will now be obtained for these models which are coupled at the edge of the coastal zone. The procedure in outline is as follows:

1) Specify the streamfunction at the edge of the coastal zone on all boundaries except the western boundary from solutions of the coastal zone equation driven by the local longshore windstress.

2) Use these boundary conditions, together with the wind curl forcing, to obtain the interior solution.

3) Use the streamfunction at the edge of the coastal zone on the western boundary from the interior solution, together with the local longshore wind stress, to obtain the solution in the coastal zone of the western boundary.

4. Solutions in the ocean interior

a. *The boundary condition*

From the results for eastern and zonal boundaries of Sections 5b1 and 5b2, we have that the local coastal transport due to the longshore wind stress is of O($\tau_{wl}/\rho_0\beta$). Thus the boundary streamfunction for the interior solution is

$$\psi(l) \approx -\frac{1}{\rho_0\beta}\tau_{wl} + \text{constant},$$

where the longshore coordinate (l) is assumed to be directed clockwise around the ocean basin. On setting the constant to be zero, we obtain for all boundaries (except the western boundary) the approximate nondimensional boundary condition

$$\phi(l) = -F_l, \tag{14}$$

in which a proportionality constant of unity has been assumed.

The solution of (13) forced by the wind stress curl and with $\phi(l) = 0$, has been extensively discussed elsewhere; it will not be considered here except as part of the total solution for the South Indian Ocean (Section 6). Our main purpose is to present solutions due to forcing by the longshore wind stress along the eastern and zonal boundaries.

b. *Coastal forcing*

We consider longshore wind stress modes of the form

$$\tau_{wx} = \tau_0 \cos\frac{x}{S}, \tag{15}$$

$$\tau_{wy} = \tau_0 \cos\frac{y}{S}, \tag{16}$$

in which, consistent with Section 3b,

$$\left(\frac{W}{S}\right)^2 \ll 1. \tag{17}$$

Then for a wide range of scales of forcing, typical of the structure of the longshore wind imparted by the coastal geometry in real ocean basins, it is found that the solutions associated with each boundary may be treated separately, since they give rise to relatively small perturbations in streamfunction on the other boundaries.

1) EASTERN BOUNDARY

On nondimensionalizing (16), we obtain

$$F_y = \cos(\alpha Y),$$

where $\alpha = LS^{-1}$, and hence from (14) the boundary condition on the eastern boundary ($X = 1$) is

$$\phi(1, Y) = -\cos(\alpha Y). \tag{18}$$

The exact solution of (13) which satisfies (18) is easily found to be

$$\phi = -\left(\frac{e^{\lambda_1 X} - e^{\lambda_2 X}}{e^{\lambda_1} - e^{\lambda_2}}\right)\cos(\alpha Y),$$

where

$$\lambda_1 = \frac{-1 + (1 + 4\epsilon^2\alpha^2)^{1/2}}{2\epsilon},$$

$$\lambda_2 = \frac{-1 - (1 + 4\epsilon^2\alpha^2)^{1/2}}{2\epsilon}.$$

For large-scale forcing which satisfies the inequality (17), we have $(\epsilon\alpha)^2 \ll 1$, and the solution simplifies in the ocean interior to the form

$$\phi = -e^{-\epsilon\alpha^2(X-1)}\cos(\alpha Y), \quad (\epsilon\alpha)^2 \ll 1, \qquad (19)$$

which is an exact solution of the reduced vorticity equation

$$\frac{\partial\phi}{\partial X} + \epsilon\frac{\partial^2\phi}{\partial Y^2} = 0. \qquad (20)$$

For wind stress curl forcing, the interior solution behaves in an analogous manner (Bye and Veronis, 1979).

Eq. (19) represents a flowfield in which the transport in the coastal boundary current is partially compensated by a return flow in a series of parallel coastal zonal waves in the interior, and partially by the western boundary current. For long-wavelength forcing ($\epsilon\alpha^2 \to 0$), $\phi \to -\cos(\alpha Y)$, and hence the interior flow is suppressed, and all the return flow occurs in the western boundary current. For short-wavelength forcing ($\epsilon\alpha^2 \gtrsim 1$), however, the compensating deep ocean current occurs mainly in the interior (Fig. 2). The dimensional decay length is $\beta S^2/R$, e.g.; for $S = 300$ km, $R = 10^{-6}$ s^{-1}, $\beta = 2 \times 10^{-11}$ m^{-1} s^{-1} we obtain 500 km.

2) Zonal boundary

On nondimensionalizing (15) we obtain

$$F_x = \cos(\alpha X),$$

and hence the boundary condition on the southern boundary ($Y = 0$) is

$$\phi(X, 0) = -\cos(\alpha X). \qquad (21)$$

For large-scale forcing in the ocean interior, the approximate solution of (13) which satisfies (21) is

$$\phi = -\exp[-(\alpha/2\epsilon)^{1/2}Y]\cos[\alpha X + (\alpha/2\epsilon)^{1/2}Y], \quad (\epsilon\alpha)^2 \ll 1. \qquad (22)$$

This solution which also is an exact solution of (20) represents a series of parallel crested stationary waves the orientation of which lies west of north at an angle

$$\theta = \tan^{-1}(2\epsilon\alpha)^{1/2}$$

to the coast, and which decay into the basin (Fig. 2). Similarly for a northern boundary ($Y = Y_0$), on assuming that

$$F_x = \cos(\alpha X),$$

we obtain the solution

$$\phi = -\exp[(\alpha/2\epsilon)^{1/2}(Y - Y_0)] \times \cos[\alpha X - (\alpha/2\epsilon)^{1/2}(Y - Y_0)], \quad (\epsilon\alpha)^2 \ll 1, \qquad (23)$$

which represents parallel crested waves, the orienta-

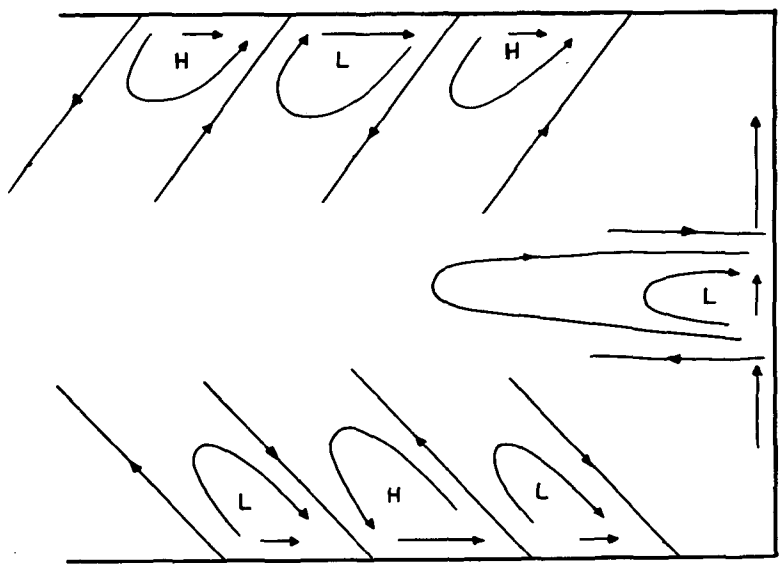

FIG. 2. Coastal waves.

tion of which lies west of south, at an angle θ to the coast (Fig. 2).

These waves have some interesting properties. First, the nondimensional decay length is $(2\epsilon/\alpha)^{1/2}$, which by virtue of the inequality (17) is of scale intermediate between that of the forcing α^{-1}, and of the western boundary current ϵ. In dimensional terms, the decay length is $(2RS\beta^{-1})^{1/2}$, e.g., for $S = 300$ km, $R = 10^{-6}$ s^{-1}, $\beta = 2 \times 10^{-11}$ m^{-1} s^{-1}, the western boundary current width is 50 km and the decay length 200 km. Second, the waves lie at an angle to the coast, consistent with the flow of momentum from the coastally induced current into the deep ocean. The steady nonlinear deep ocean current which results, to a first approximation, is

$$u' = -\frac{1}{R}\frac{\partial}{\partial y}\widehat{uv},$$

where the caret denotes an average of a wavelength of the coastal forcing, over which a momentum balance normal to the coastline is assumed. Since $\widehat{uv} > 0$ for a northerly coast, and $\widehat{uv} < 0$ for a southerly coast, $u' < 0$, and on integrating across the current, using (22) or (23), we find that the magnitude of the westward nonlinear transport,

$$T = \frac{1}{h_T}\left(\frac{\tau_0}{\rho_0}\right)^2 (2SR\beta)^{-3/2}, \quad \left(\frac{W}{S}\right)^2 \ll 1, \qquad (24)$$

which is most significant for short-wavelength forcing.

The sets of coastal waves represented by (19), (22) and (23) are important features of the oceanic general circulation, which describe circulation patterns on a scale intermediate between that of boundary currents and the major oceanic gyres. The primary process involved is the loss of momentum from the sea surface, a large-scale process that does not depend intimately on local topography. The coastal currents and the coastal waves are complementary phenomena occurring respectively along the boundary and within the interior of the ocean basin, and consequently are of similar transport.[1] The nonlinear transport associated with the coastal waves may oppose or reinforce the coastal current. On assuming that the transport scale for the coastal current is $\tau_{wl}/\rho_0\beta$, typical transport magnitudes in the coastal waves would be 5 Sv and assuming that $S = 300$ km, the nonlinear transport (24) would be 1 Sv.[2] A linear superposition of the coastally forced solutions can satisfy an arbitrary longshore wind stress distribution.

[1] It is suggested that a suitable distinguishing name for the coastal waves would be "Stommel waves."

[2] 1 Sv = 10^6 m^3 s^{-1}.

5. Solutions in the coastal zone

a. *Analytical solutions*

On the inner shelf the approximate steady-state balance of terms (*cf.* Bye 1983b) in (1) and (2) is

$$\tau_{wl} \approx \rho_0 C_0 u(l),$$

where l is the longshore coordinate, from which an approximate expression for the nondimensional current at the edge of the inner shelf is

$$U(l) = F_l/\epsilon, \qquad (25)$$

which is of the same order as the western boundary current. We consider now the solutions on the outer shelf.

1) THE WESTERN BOUNDARY

On the outer shelf ($H = 1$), Eq. (12) reduces to

$$V = -\epsilon\frac{\partial V}{\partial X} + \epsilon^3\frac{\partial^3 V}{\partial X^3}. \qquad (26)$$

The solution of (26) with the boundary conditions

$$V = \begin{cases} \dfrac{\partial V}{\partial X} = 0, & X \to \infty \\ \dfrac{F_l}{\epsilon}, & X = 0, \end{cases}$$

such that the current decays to zero in the deep ocean, and equals the coastal current (25) at the edge of inner shelf ($X = 0$), may be obtained by assuming a trial solution of the form $\epsilon^{mX/\epsilon}$ from which we obtain the cubic indicial equation

$$m^3 - m = 1,$$

which has the roots

$$m_1 = \lambda, \quad m_2 = -\frac{\lambda}{2} + i\nu, \quad m_3 = -\frac{\lambda}{2} - i\nu, \qquad (27)$$

where $\lambda = 1.325$ and $\nu = 0.526$. The western boundary solution, derived from the roots (m_2, m_3), is

$$V = \frac{A}{\epsilon}e^{-\lambda X/2\epsilon} \times [F_l\cos(\nu X\epsilon^{-1} + B) + \nu A\phi_0 \sin\nu X\epsilon^{-1}], \qquad (28)$$

where $A = [1 + (\lambda/2\nu)^2]^{1/2}$ and $B = \tan^{-1}(\lambda/2\nu)$. This solution consists of two parts: the first which has a zero transport is due to the longshore wind stress (F_l); and the second which has zero velocity at $X = 0$ is due to the prescribed interior transport (ϕ_0) at the edge of the coastal zone, where

$$\phi_0 = \phi_I + \phi_E + \phi_S + \phi_N,$$

in which the streamfunctions ϕ_I, ϕ_E, ϕ_S and ϕ_N are due respectively to wind stress curl forcing, and

coastal current forcing on the eastern, southern, and northern boundaries, the coastal forcing normally being of lesser importance. Both parts of the solution are decaying exponentials, the second part being of similar form to the classical solution of Munk (1950) in which $\lambda = 1$ and $\nu = 0.866$. The ratio of the wavelength to the decay length of the solution ($\pi\lambda/\nu$) is 7.4 for our solution, and 3.6 for Munk's solution, and thus the transport oscillation is significantly less, and the maximum transport is $1.02\phi_0$ whereas Munk's solution predicts $1.17\phi_0$. The coastal current on the western boundary due to longshore wind is fundamentally different from that on the other boundaries which have nonzero transports (*cf.* Section 5a2).

2) THE EASTERN AND ZONAL BOUNDARIES

From (26), the eastern boundary solution, which results from the single root (m_1), and satisfies the boundary conditions

$$V = \begin{cases} \dfrac{\partial V}{\partial X} = 0, & X \to -\infty \\ \dfrac{F_l}{\epsilon}, & X = 1, \end{cases}$$

is

$$V = \frac{F_l}{\epsilon} e^{\lambda(X-1)/\epsilon}, \tag{29}$$

and on integrating across the outer shelf we obtain the eastern coastal transport F_l/λ.

For a zonal boundary, the equation for the outer shelf derived in the same manner as (26) is

$$0 = -\epsilon \frac{\partial U}{\partial Y} + \epsilon^3 \frac{\partial^3 U}{\partial Y^3},$$

the solution of which for a southern boundary with the boundary conditions

$$U = \begin{cases} \dfrac{\partial U}{\partial Y} = 0, & Y \to \infty \\ \dfrac{F_l}{\epsilon}, & Y = 0 \end{cases}$$

is

$$U = \frac{F_l}{\epsilon} e^{-Y/\epsilon}, \tag{30}$$

the solution for the northern boundary being the corresponding expression

$$U = \frac{F_l}{\epsilon} e^{(Y-Y_0)/\epsilon}. \tag{31}$$

Thus on integrating across the outer shelf, the zonal coastal transport is F_l.

b. Numerical solutions for an exponential shelf

1) THE WESTERN BOUNDARY

A series of numerical solutions of (12) have been obtained for the exponential shelves

$$H = \begin{cases} e^{X/\gamma}, & X_0 \leqslant X \leqslant 0 \\ 1, & 0 \leqslant X \leqslant X_1, \end{cases}$$

where $X = 0$ marks the edge of the inner shelf, with the boundary conditions,

$$V = \begin{cases} 0 \quad \text{at} \quad X = X_0 \\ \dfrac{\partial V}{\partial X} = 0 \quad \text{at} \quad X = X_1, \end{cases} \tag{32}$$

in which γ is the nondimensional shelf width, which is typically $O(\epsilon)$. For the exponential shelf, on substituting $\zeta = -X\gamma^{-1}$ the vorticity equation may be written

$$\begin{aligned} \phi_\zeta \sigma^2(-H\sigma + 1) &= \sigma^2 F_l + (H - \sigma^2)\phi_{\zeta\zeta} \\ &\quad - 2H\phi_{\zeta\zeta\zeta} + H\phi_{\zeta\zeta\zeta\zeta}, \quad H < 1, \\ -\sigma^3\phi_\zeta &= -\sigma^2\phi_{\zeta\zeta} + \phi_{\zeta\zeta\zeta\zeta}, \quad H = 1, \end{aligned} \tag{33}$$

in which $\sigma = \gamma/\epsilon$ and $V = \phi_\zeta/\epsilon$. Thus the solutions are determined by the single parameter σ which is small if γ is a small (narrow shelf) and large if γ is a large (wide shelf) compared with the boundary layer width.

We have investigated the circulation for several values of σ for the segment ($\zeta_1 = -8$, $\zeta_0 = 4$). A finite difference representation of (33) together with the boundary conditions (32) has been solved with the grid interval $\Delta\zeta = 0.1$. Two solutions have been obtained for each σ, corresponding to coastal forcing by the longshore wind, and forcing by the imposed transport.

Two types of solution were found. For narrow shelves the transport forced solution has maximum currents near the edge of the inner shelf, and the coastally forced solution has a current maximum on the inner shelf (Fig. 3). For wide shelves, however, the current maximum of the transport forced solution occurs beyond the edge of the inner shelf, with a countercurrent inshore; the coastally forced solution has two current maxima, one inshore and the other beyond the inner shelf edge, with an intermediate countercurrent maximum (Fig. 4). These two circulation modes indicate the possibility of a shift in the axis of the boundary current such that it occurs over the inner shelf for narrow shelves, but on wider shelves it is separated from the inner shelf with a countercurrent closer inshore.

The series of solutions indicate that the transition occurs in the parameter range $0.7 < \sigma < 2.0$. For $\sigma \leqslant 0.7$ only the narrow shelf solution type occurs, whereas for $\sigma \geqslant 2.0$ only the wide shelf solution type occurs. Within the transition range some values of σ give narrow and some wide shelf type solutions. This behavior is characteristic of boundary currents in the real ocean; however, the one-dimensional model is too simple for detailed inferences to be made.

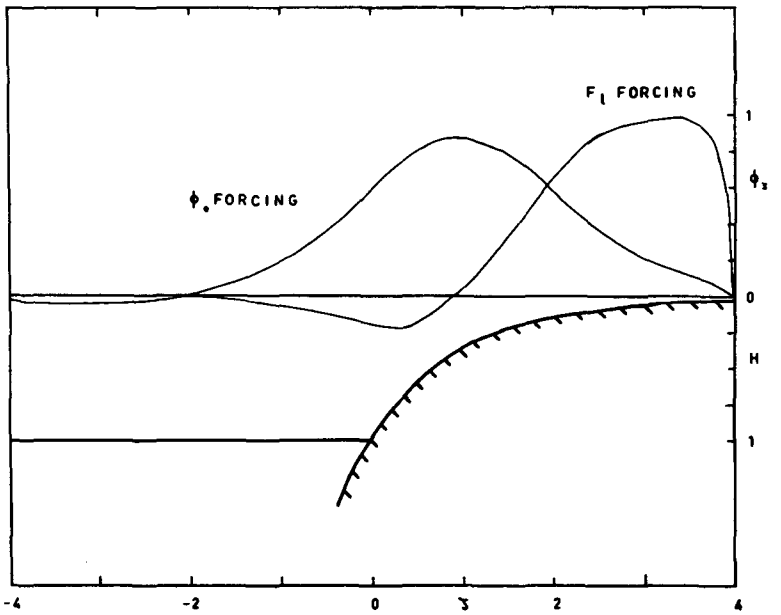

FIG. 3. The nondimensional profiles of velocity adjacent to the westerly coast for an exponential shelf parameter $\sigma = 1$ due to forcing by the deep ocean transport, and the longshore wind stress on the inner continental shelf.

2) THE EASTERN AND ZONAL BOUNDARIES

A series of solutions for exponential shelves of various widths (Bye, 1983b) show that the coastal transport on eastern and zonal boundaries over a wide range of shelf widths is of $O(F_l)$, in agreement with the analytical estimates of Section 5a2; the corresponding dimensional transport being of $O(\tau_{wl}/\rho_0\beta)$, which has a typical magnitude of 5 Sv.

6. The South Indian Ocean circulation

The formulations of Section 3 have been applied to the circulation in the South Indian Ocean which is represented between latitudes 15°S and 45°S, and longitudes 85°E and 145°E, by a rectangular geometry (Fig. 5). The longitudinal and latitudinal dimensions of the exterior rectangle are 6000 and 3000 km, respectively, and land boundaries are supposed to

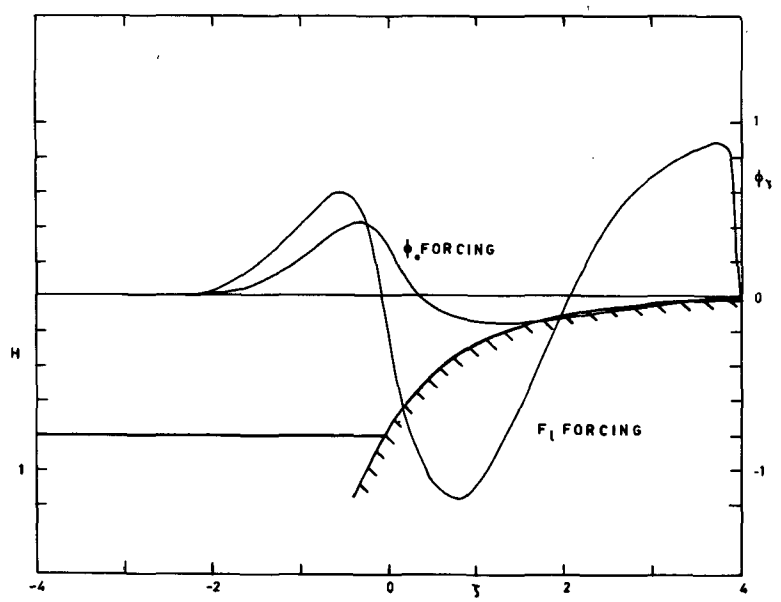

FIG. 4. The nondimensional profiles of velocity adjacent to the westerly coast for an exponential shelf parameter, $\sigma = 2.5$ due to forcing by the deep ocean transport, and the longshore wind stress on the inner continental shelf.

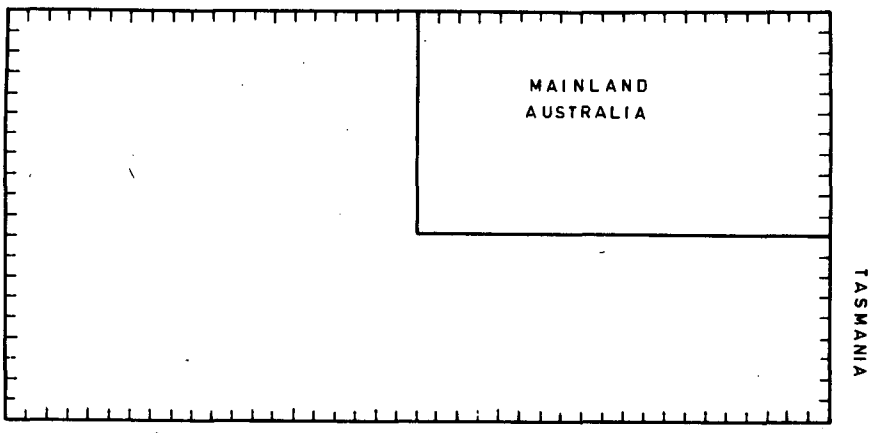

FIG. 5. The eastern South Indian Ocean model.

exist around its perimeter, and also on the perimeter of a rectangle inset in the northwest corner of dimensions 3000 and 1800 km, respectively. This rectangle represents mainland Australia; the eastern boundary, to the south of the rectangle, represents the barrier presented by Tasmania.

The latitudinal extent of the ocean accommodates the main South Indian Ocean subtropical gyre represented by the zonal wind stress distribution

$$\tau_{wx} = \tau_0 \cos(\pi y/M),$$

where $M = 3000$ km, in which $\tau_0 = 0.1$ N m^{-2}. Along the coastline of Australia an estimate of the annual longshore wind stress distribution has been obtained using wind stress data from Eyre (1972), interpolated along the coastline with reference to the surface pressure patterns of Taljaard *et al.*, (1969), and also from an atlas of Australia. The data sources are summarized in Fig. 6, which also shows how the coastal geography was decomposed into a sequence of linear segments for the purpose of resolving the wind stress to obtain the longshore component. It is clear that the resulting longshore wind stress contains an interesting mesoscale structure resulting principally from the orientation of the coastline rather than the structure of the wind field. This is especially true off the coast of South Australia. The longshore wind distribution was finally interpolated onto the rectangular model.

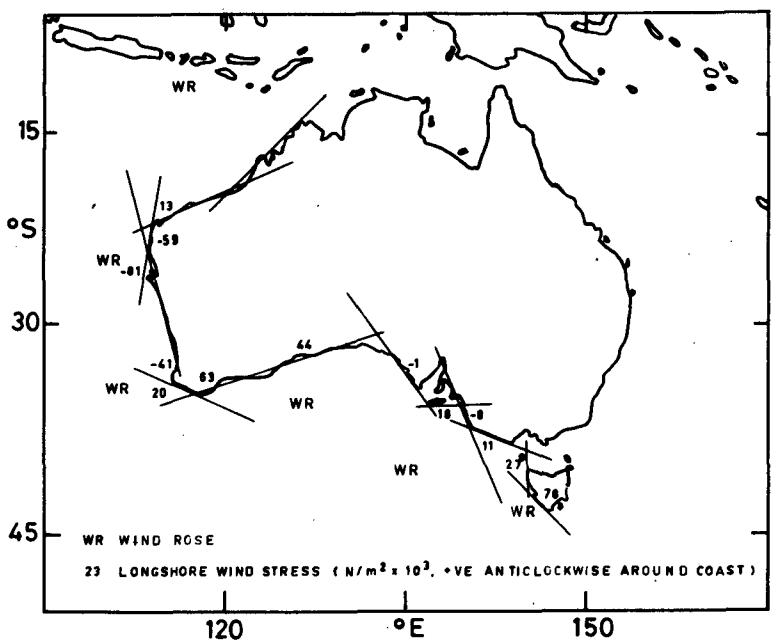

FIG. 6. Annual mean longshore wind stresses along the west and south coasts of Australia.

The nondimensional Stommel equation (13) with the boundary condition (14) on the perimeter of the ocean basin was approximated by the weighted mean finite-difference scheme of Fiadeiro and Veronis (1977) to yield

$$a_{i+1}\phi_{i+1} + a_{i-1}\phi_{i-1} + a_{j+1}\phi_{j+1} + a_{j-1}\phi_{j-1} - a_0\phi = b_0, \quad (34)$$

where

$$a_0 = a_{i+1} + a_{i-1} + a_{j+1} + a_{j-1},$$

$$a_{i+1} = \frac{1}{2k}\coth(\theta + 1), \quad a_{j+1} = \epsilon/k^2,$$

$$a_{i-1} = \frac{1}{2k}\coth(\theta - 1), \quad a_{j-1} = \epsilon/k^2,$$

$$b_0 = -\alpha \sin(\alpha Y),$$

in which k is the grid interval, $\alpha = \pi LM^{-1}$, and $\theta = k/2\epsilon$. Solutions of (34) were then obtained using $\epsilon = 0.0083$, which corresponds to a finite difference network of 41 × 21 lines for a western boundary width (W) of 50 km, and forcing due to (a) the wind stress curl only, and (b) the wind stress curl and the longshore wind stress distribution.

The streamfield (ϕ) shows clearly the importance of the longshore wind stress distribution in the total general circulation (Fig. 7). The coastal currents which close the general circulation in the coastal zone are indicated by arrows adjacent to the coasts.

The main feature of the wind stress curl forced solution is the South Indian Ocean gyre. On introducing the longshore wind stresses we differentiated this simple pattern into several subgyres which may be identified with the current features of the region. The currents which constitute the deep ocean gyre are the Flinders Current to the south of Australia, and the West Australian Current to the west of Australia. The structure of the Flinders Current includes the following.

1) A recirculation off southwest Australia due to the eastward transport of the coastal Leeuwin Current which flows around Cape Leeuwin and into the Great Australian Bight. The deep ocean recirculation which reinforces the westward flow of the global forcing of the Flinders Current, the total transport being about 8 Sv.

2) A series of coastal waves of short wavelength induced by the coastal geography of South Australia, which extend southwestward beyond 40°S.

3) A convergence of deep ocean streamlines along the west coast of Tasmania due to the Zeehan Current which flows eastward around the south of Tasmania.

The intermediate-scale geostrophic structure off South Australia was observed in a repeated series of cruises over the period 1967–71 (Bye, 1971). It is

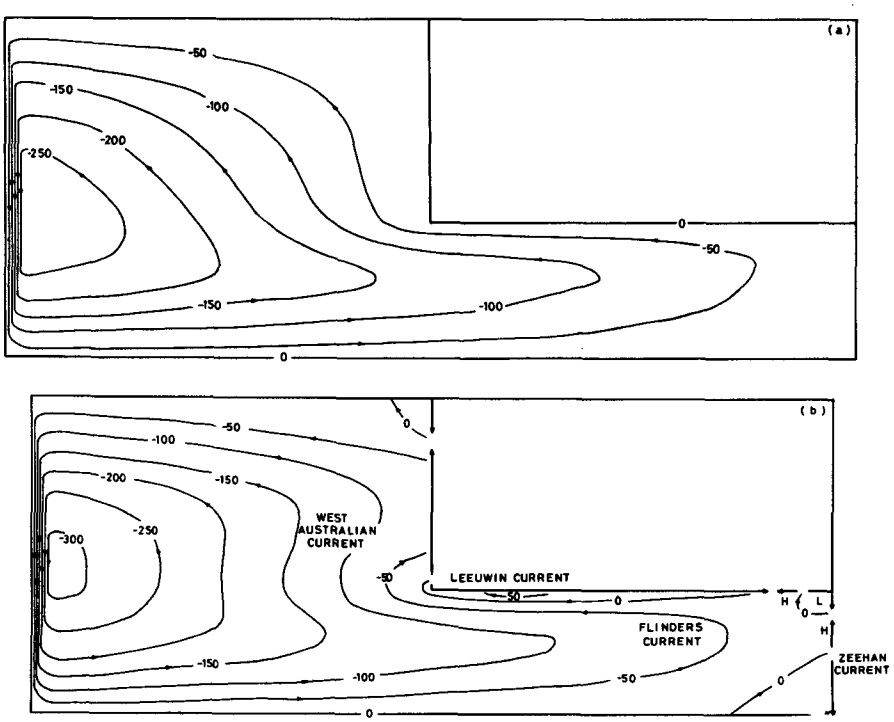

FIG. 7. The general circulation in the eastern South Indian Ocean due to forcing by (a) the wind stress curl, and (b) the wind stress curl and the longshore wind stresses. Contour unit: ($\phi \times 10^2$).

suggested that the quasi-stationary pattern (Fig. 8) obtained by averaging all station data for the period is a good example of the baroclinic structure of coastal waves. The association of the offshore and onshore geostrophic flows in Fig. 8[3], with changes of orientation of the coastline in a manner consistent with forcing by changes in coastal transport is quite remarkable. The system of transport convergences and divergences persists throughout the year due to the wind field in this region which is westerly in winter, and southeasterly in summer (Bye, 1983a). The geometry of Fig. 7 cannot be expected to resolve the wave structure. Accordingly, an additional solution (13) adjacent to a northeastern boundary, approximating the mean orientation of the South Australian and Victorian coastlines (Fig. 6), was solved for a coastal forcing consisting of two wavelengths of 800 km in a rectangular region of dimensions 1600 km $\times$ 1000 km on a finite-difference network of 33 lines $\times$ 21 lines with $\epsilon = 0.031$. Coastal waves were found with a decay length of about 250 km, and with their crests oriented approximately east-northeast. On superimposing a uniform current parallel to the coast we obtained a streamline pattern similar to the observed baroclinic transport topography (Fig. 8) in which a high lies to the southwest, and ridges extend toward the coast between closed regions of low topography (Fig. 9).

Thus the intermediate-scale structure of the Flinders Current can be reproduced by a series of coastal waves superimposed on a large-scale westward gyral current. The magnitude of the transport of the coastal waves at the coast predicted from the coastal wind field is about 2 Sv; the observed baroclinic transport in the waves at the coast, however, is about 8 Sv (Fig. 8).

The reason for this difference may be that a transverse disturbance of wavelength 800 km superimposed on the westward large-scale flow is baroclinically unstable. The resulting baroclinic structure of the coastal waves would then represent an equilibrium amplitude for the instability mechanism. Under these circumstances, the nonlinear coastal transport may be an important feature; this conjecture requires further study. Thus conditions are particularly favorable for the onset of a strong Flinders Current south of South Australia, since the westward gyral transport would be enhanced by the nonlinear current.

The observed transport magnitude of about 10 Sv (Fig. 8) may reflect approximately equal contributions from the gyral and the nonlinear transports. In summer, the direct wind-driven coastal current also flows in the same direction as the gyral transport.

Off southwest Australia, a northeast trending flow

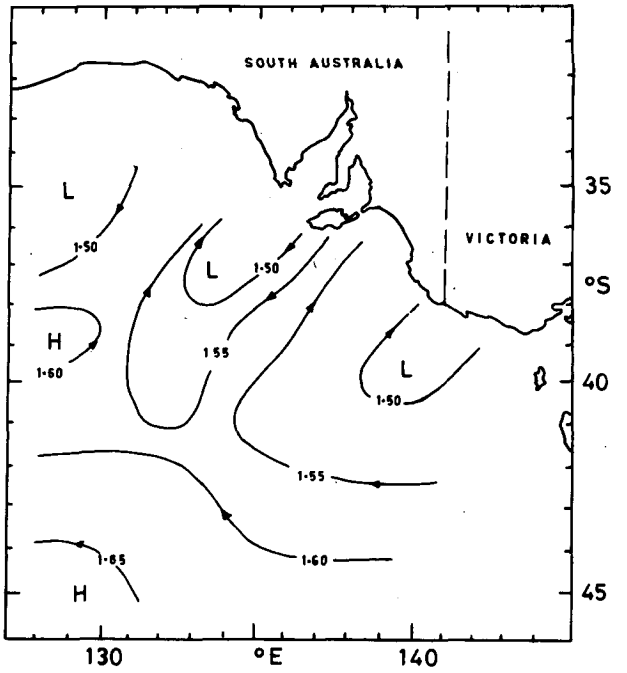

FIG. 8. The surface anomaly of potential energy relative to 2000 db south of South Australia. Contour units: (dyn m)^2.

in the deep ocean is observed (Andrews, 1977), and it is interesting to note that the deep ocean gyre and the annual mean coastal current along the central West Australian coastline have the same orientation. Strong seasonal changes associated with the southward propagation of the Leeuwin Current occur however (Godfrey, 1983). The Zeehan Current off western Tasmania is discussed in Baines *et al.* (1983). The western boundary current which closes the main ocean gyre is notional rather than geographical.

Thompson and Veronis (1983) have already discussed the circulation of the South Indian Ocean, with particular reference to the Leeuwin Current. The wind stress curl in their model was allowed to adjust so that meridional winds existed along the west coast of Australia. However, no attempt was made to reproduce the details of the longshore wind stress distribution as in this study. Significant effects on the general circulation of the coastal currents were also found.

7. Conclusion

It has been shown that the inclusion of a homogeneous frictional process within the interior of the ocean leads to a class of free waves which form part of the general circulation. These frictional waves have been called coastal waves. The coastal wavefield can be predicted from the longshore wind stress distribution around the perimeter of the ocean basin, together with information on the shelf geometry. Although only a rectangular basin has been considered, the representation of the frictional processes implies that boundary layers of width $W \approx C_0/h_T\beta$ would

[3] The reader should note that Fig. 8 was drawn many years before this study was commenced. Originally, the waves were thought to be Rossby waves supported on an eastward flowing deep current.

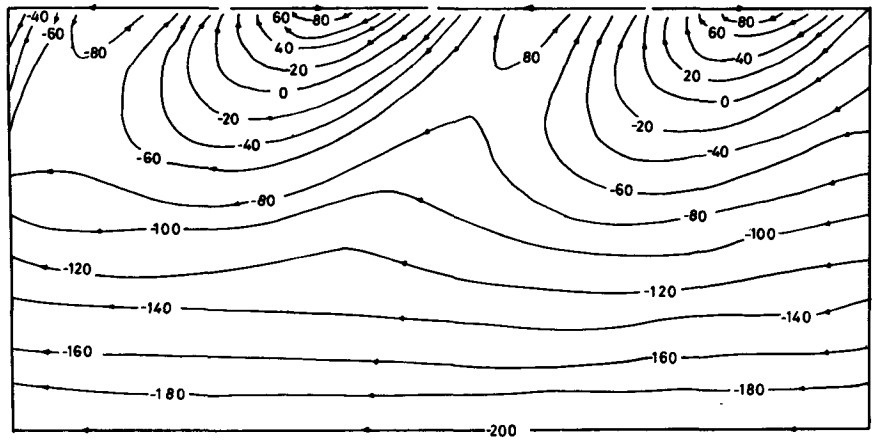

FIG. 9. The circulation adjacent to a northeastern boundary due to longshore wind stress forcing of wavelength 800 km, with the addition of a uniform transport parallel to the coastline.

exist adjacent to any coastline. Since potential vorticity is approximately conserved across high-velocity (inertial) baroclinic streams, classical arguments (Stommel, 1965) lead to the independent estimate of boundary layer width,

$$W \approx \left(\frac{g\Delta\rho}{\rho_0} h_T\right)^{1/2} \Big/ |f|,$$

where $\Delta\rho$ is the density difference between the two layers of the baroclinic model, which also is only weakly dependent on coastal orientation. The two estimates for W, however, are mutually consistent since they may always be solved for $h_T(x, y)$ which is a free parameter in both arguments.

It would be interesting to examine the longshore wind stress distribution along the length of the world ocean coastline to determine all regions where coastal waves would be especially prominent, taking into account the annual mean wind field and seasonal change. For example, southern California and Europe both have a sharp intermediate scale coastline geography. The nonlinear current would reinforce the equatorial circuit of the main ocean gyres, but oppose the polar circuit.

The solution for the western boundary, including the continental shelf, shows that the velocity structure in the boundary current is sensitive to the shelf width. Thus there is the possibility of a sudden displacement of the main stream on encountering a wide shelf. This feature may be significant in understanding the dynamics of the Gulf Stream and other boundary currents. The longshore wind stress on the western boundary drives no net transport; however, appreciable currents may be generated in the coastal zones. The onset of the Somali Current, for example, is perhaps associated initially with the onset of a longshore wind stress, rather than with the change in the wind stress curl in the North Indian Ocean.

Time-dependent motions have not been considered. All coastal wind variability of frequency much less than the friction decay constant, i.e., $R \ll 0.1$ day^{-1}, however, would allow almost complete adjustment of the coastal transports (Bye, 1983b), and thus induce an important time-dependent response in the ocean interior. The resulting low-frequency coastal waves would be almost horizontally nondivergent, and it would be interesting to examine their structure using a quasi-geostrophic model forced by flow in the surface layer ($h < h_T$) normal to the boundary.

REFERENCES

Andrews, J. C., 1977: Eddy structure and the West Australian Current. *Deep-Sea Res.*, **24**, 1133–1148.

Baines, P. G., R. J. Edwards and C. B. Fandry, 1983: Observations of a new baroclinic current along the western continental slope of Bass Strait. *Aust. J. Mar. Freshwater Res.*, **34**, 155–157.

Bye, J. A. T., 1971: Variability south of Australia. *Proc. Int. Mar. Sci. Symp.*, Sydney, Australia, 119–135.

——, 1980: Energy dissipation by the large scale circulation. *Ocean Model.*, **31**, 12–13 (unpublished manuscript).

——, 1983a: Physical oceanography of the south-east coastal waters. *Natural History of the South East.* Roy. Soc. S. Aust. (in press).

——, 1983b: On the definition of a coastal current. (submitted to *Estuarine Coastal Mar. Sci.*).

——, and G. Veronis, 1979: A correction to the Sverdrup transport. *J. Phys. Oceanogr.*, **9**, 649–651.

Eyre, W. S., 1972: The spherical harmonic analysis of global wind stress field and atmospheric angular momentum. Res. Rep. No. 6, Flinders Institute for Atmospheric and Marine Sciences, The Flinders University of South Australia.

Fiadeiro, M. E., and G. Veronis, 1977: On weighted-mean schemes for the finite-difference approximation to the advection-diffusion equation. *Tellus*, **29**, 512–522.

Godfrey, J. S., 1983: Notes on the physics of the Leeuwin Current. *Aust. J. Mar. Freshwater Res.* (in press).

Munk, W. H., 1950: On the wind-driven ocean circulation. *J. Meteor.*, **7**, 79–93.

Stommel, H. 1965: *The Gulf Stream.* California University Press, 248 pp.

Taljaard, J. J., H. van Loon, H. L. Crutcher and R. L. Jenne, 1969: Climate of the upper air. Part 1. Southern Hemisphere. NCAR, Washington D.C.

Thompson, R. O. R. Y., and G. Veronis, 1983: Poleward boundary current off Western Australia. *Aust. J. Mar. Freshwater Res.*, **34**, 173–185.